
Supplementary Information

Beyond Equilibrium: Kinetic Thresholds and Rheological
Feedbacks Control 410 Topography

Kerswell B., Wheeler J., Gassmöller R., Davies, J.H.

24 November 2025

Measuring 410 Displacement and Width

Structure of the 410 was evaluated from the volume fraction field X along vertical profiles that intersected either: 1) the widest phase transition zone or 2) the largest displacement of the olivine \Leftrightarrow wadsleyite reaction found within model domain. The phase transition zone width was defined as the difference between the depths at $X = 0.9$ and $X = 0.1$, while the olivine \Leftrightarrow wadsleyite reaction displacement was defined as the offset between the nominal equilibrium reaction depth and the depth at $X = 0.9$. The exact vertical profile position was chosen heuristically by “best fit” criteria based on structural characteristics of the phase transition zone. The maximum reaction rate \dot{X} and vertical velocity \vec{u}_y were evaluated along the selected vertical profile, within the upper and lower bounds of the phase transition zone, after 100 Ma of evolution. Selected examples of vertical profile picking in slab simulations are shown in Figure 1.

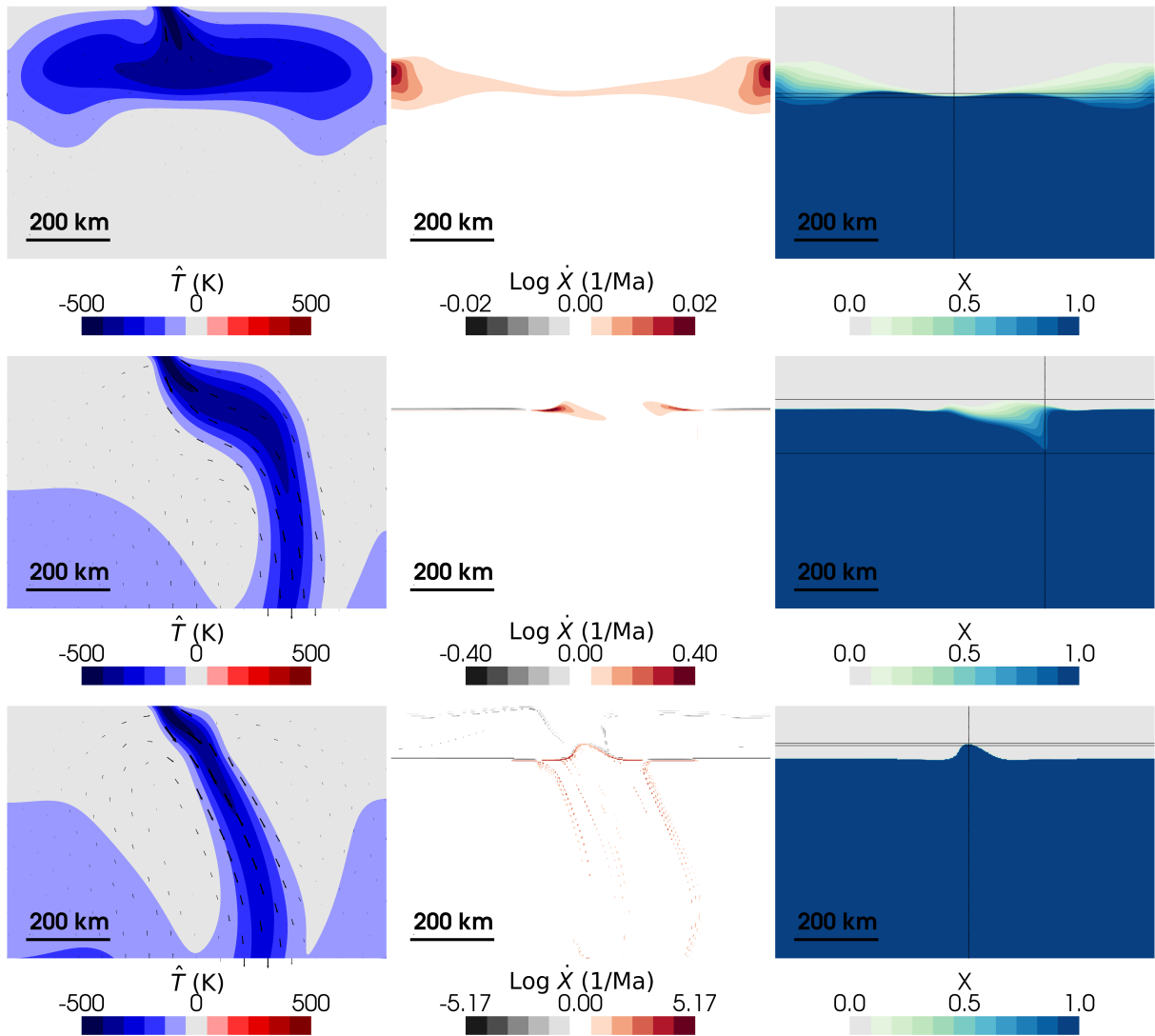


Figure 1: Slab simulations with intermediate strength contrasts ($B = 4$) demonstrating ultra-sluggish (top row: $Z = 3.0 \text{e}0 \text{ K s}^{-1}$), intermediate (middle row: $Z = 4.7 \text{e}2 \text{ K s}^{-1}$), and quasi-equilibrium (bottom row: $Z = 7.0 \text{e}7 \text{ K s}^{-1}$) kinetic regimes after 100 Ma evolution. Panels show dynamic temperature \hat{T} (left column), reaction rate \dot{X} (middle column), and volume fraction of wadsleyite X (right column). Thin black lines indicate the vertical profile and depth bounds for measuring 410 structure (width and displacement).

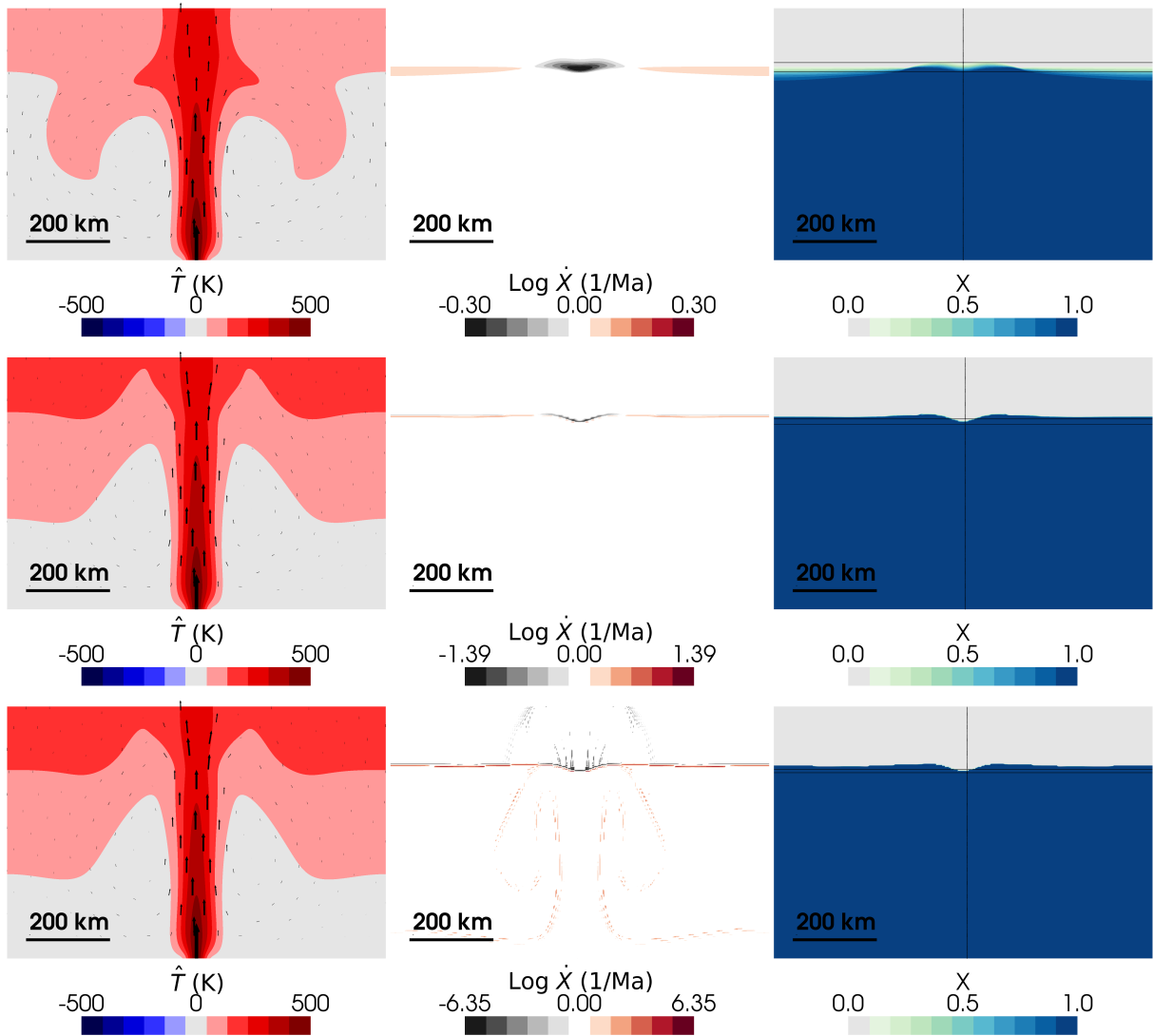


Figure 2: Plume simulations with intermediate strength contrasts ($B = 4$) demonstrating ultra-sluggish (top row: $Z = 3.0 \times 10^0 \text{ K s}^{-1}$), intermediate (middle row: $Z = 4.7 \times 10^2 \text{ K s}^{-1}$), and quasi-equilibrium (bottom row: $Z = 7.0 \times 10^7 \text{ K s}^{-1}$) kinetic regimes after 100 Ma evolution. Panels show dynamic temperature \hat{T} (left column), reaction rate \dot{X} (middle column), and volume fraction of wadsleyite X (right column). Thin black lines indicate the vertical profile and depth bounds for measuring 410 structure (width and displacement).

Table 1: Summary of the kinetic prefactor Z , rheological activation factor B , 410 structure (displacement and width), maximum vertical velocity \vec{u}_y , and maximum reaction rate \dot{X} evaluated in plume and slab simulations after 100 Ma of evolution. Units are Z : K s^{-1} , B : none, displacement: km, width: km, \vec{u}_y : cm/yr , $\log_{10} \dot{X}$: $\log_{10} \text{Ma}^{-1}$.

Simulation	Z	B	Displacement	Width	Max \vec{u}_y	$\log_{10} \text{Max } \dot{X}$
plume	3.0e0	2	20	19	1.71	-0.01
plume	3.0e0	4	20	19	1.78	-0.01
plume	3.0e0	6	19	20	1.85	-0.01
plume	3.0e0	8	19	21	1.91	-0.01
plume	3.0e0	10	18	21	1.96	-0.01
plume	7.0e0	2	21	14	2.06	0.2
plume	7.0e0	4	21	15	2.19	0.21
plume	7.0e0	6	20	15	2.32	0.22
plume	7.0e0	8	20	16	2.45	0.22
plume	7.0e0	10	19	17	2.58	0.22
plume	1.6e1	2	22	10	2.29	0.39
plume	1.6e1	4	22	11	2.46	0.41
plume	1.6e1	6	21	12	2.65	0.42
plume	1.6e1	8	21	12	2.84	0.42
plume	1.6e1	10	20	12	3.04	0.44
plume	3.7e1	2	23	8	2.42	0.59
plume	3.7e1	4	23	8	2.62	0.61
plume	3.7e1	6	22	8	2.85	0.61
plume	3.7e1	8	22	9	3.09	0.61
plume	3.7e1	10	21	9	3.34	0.64
plume	8.7e1	2	24	6	2.53	0.76
plume	8.7e1	4	24	6	2.76	0.75
plume	8.7e1	6	23	7	3	0.8
plume	8.7e1	8	23	7	3.29	0.84

Simulation	Z	B	Displacement	Width	Max \vec{u}_y	$\log_{10} \text{Max } \dot{X}$
plume	8.7e1	10	22	7	3.58	0.86
plume	2.0e2	2	24	4	2.57	0.97
plume	2.0e2	4	24	5	2.84	0.94
plume	2.0e2	6	24	6	3.07	0.89
plume	2.0e2	8	24	6	3.38	0.98
plume	2.0e2	10	23	6	3.72	1.04
plume	4.7e2	2	24	3	2.59	1.19
plume	4.7e2	4	24	4	2.85	1.13
plume	4.7e2	6	24	4	3.14	1.07
plume	4.7e2	8	24	4	3.48	1.04
plume	4.7e2	10	24	5	3.74	1.1
plume	1.1e3	2	24	3	2.65	1.42
plume	1.1e3	4	24	3	2.87	1.3
plume	1.1e3	6	24	3	3.15	1.26
plume	1.1e3	8	24	4	3.51	1.19
plume	1.1e3	10	24	4	3.86	1.14
plume	2.6e3	2	24	3	2.79	1.6
plume	2.6e3	4	24	3	2.91	1.5
plume	2.6e3	6	24	3	3.23	1.44
plume	2.6e3	8	24	3	3.46	1.5
plume	2.6e3	10	24	4	3.92	1.27
plume	6.0e3	2	24	2	2.5	1.63
plume	6.0e3	4	24	3	2.88	1.93
plume	6.0e3	6	24	3	3.29	1.65
plume	6.0e3	8	24	3	3.47	1.86
plume	6.0e3	10	24	4	3.88	1.63
plume	1.4e4	2	24	2	2.51	1.7

Simulation	Z	B	Displacement	Width	Max \vec{u}_y	$\log_{10} \text{Max } \dot{X}$
plume	1.4e4	4	24	3	2.82	2.03
plume	1.4e4	6	24	2	3.09	1.68
plume	1.4e4	8	24	3	3.55	2.11
plume	1.4e4	10	24	4	3.89	2.02
plume	3.3e4	2	24	2	2.42	1.82
plume	3.3e4	4	24	2	2.63	1.66
plume	3.3e4	6	24	3	2.99	2.3
plume	3.3e4	8	24	3	3.63	2.36
plume	3.3e4	10	24	3	4.03	2.21
plume	7.8e4	2	24	2	2.06	1.64
plume	7.8e4	4	24	3	2.9	2.67
plume	7.8e4	6	24	2	2.89	2.06
plume	7.8e4	8	24	3	3.53	2.9
plume	7.8e4	10	24	3	5.33	2.44
plume	1.8e5	2	24	2	2.06	1.96
plume	1.8e5	4	24	3	2.88	3.08
plume	1.8e5	6	24	2	2.93	2.52
plume	1.8e5	8	24	3	3.51	3.28
plume	1.8e5	10	24	2	4.26	2.65
plume	4.3e5	2	24	2	2.06	2.34
plume	4.3e5	4	24	3	2.87	3.48
plume	4.3e5	6	24	2	3.24	2.93
plume	4.3e5	8	24	3	3.51	3.66
plume	4.3e5	10	24	3	4.18	3.13
plume	1.0e6	2	24	2	2.06	2.71
plume	1.0e6	4	24	3	2.87	3.85
plume	1.0e6	6	24	2	3.23	3.31

Simulation	Z	B	Displacement	Width	Max \vec{u}_y	$\log_{10} \text{Max } \dot{X}$
plume	1.0e6	8	24	3	3.51	4.03
plume	1.0e6	10	24	3	4.19	3.48
plume	2.4e6	2	24	2	2.06	3.09
plume	2.4e6	4	24	3	2.87	4.24
plume	2.4e6	6	24	2	3.22	3.7
plume	2.4e6	8	24	3	3.51	4.41
plume	2.4e6	10	24	3	4.21	3.83
plume	5.6e6	2	24	2	2.06	3.46
plume	5.6e6	4	24	3	2.86	4.61
plume	5.6e6	6	24	2	3.22	4.08
plume	5.6e6	8	24	3	3.51	4.77
plume	5.6e6	10	24	2	4.24	4.17
plume	1.3e7	2	24	2	2.05	3.83
plume	1.3e7	4	24	3	2.86	4.98
plume	1.3e7	6	24	2	3.22	4.45
plume	1.3e7	8	24	3	3.51	5.14
plume	1.3e7	10	24	2	4.31	4.45
plume	3.0e7	2	24	2	2.05	4.19
plume	3.0e7	4	24	3	2.86	5.34
plume	3.0e7	6	24	2	3.21	4.82
plume	3.0e7	8	24	3	3.51	5.5
plume	3.0e7	10	24	2	3.71	4.05
plume	7.0e7	2	24	2	2.05	4.56
plume	7.0e7	4	24	3	2.86	5.71
plume	7.0e7	6	24	2	3.21	5.18
plume	7.0e7	8	24	3	3.51	5.87
plume	7.0e7	10	24	2	3.7	4.4

Simulation	Z	B	Displacement	Width	Max \vec{u}_y	$\log_{10} \text{Max } \dot{X}$
slab	3.0e0	2	83	7	0.09	-2
slab	3.0e0	4	85	8	0.08	-1.92
slab	3.0e0	6	88	10	0.1	-1.85
slab	3.0e0	8	91	14	0.13	-1.8
slab	3.0e0	10	95	20	0.16	-1.74
slab	7.0e0	2	66	9	0.09	-1.74
slab	7.0e0	4	69	11	0.11	-1.71
slab	7.0e0	6	73	14	0.13	-1.66
slab	7.0e0	8	78	20	0.15	-1.6
slab	7.0e0	10	84	32	0.23	-1.58
slab	1.6e1	2	50	11	0.11	-1.56
slab	1.6e1	4	54	13	0.12	-1.53
slab	1.6e1	6	60	18	0.16	-1.49
slab	1.6e1	8	144	150	0.72	-1.53
slab	1.6e1	10	167	172	0.84	-1.39
slab	3.7e1	2	38	13	0.13	-1.37
slab	3.7e1	4	45	18	0.18	-1.37
slab	3.7e1	6	144	155	1	-1.38
slab	3.7e1	8	169	179	1.09	-1.23
slab	3.7e1	10	145	154	0.99	-1.17
slab	8.7e1	2	48	32	0.29	-1.5
slab	8.7e1	4	60	49	0.46	-1.46
slab	8.7e1	6	169	183	1.34	-1.11
slab	8.7e1	8	88	101	0.91	-0.99
slab	8.7e1	10	57	70	0.72	-0.97
slab	2.0e2	2	158	184	1.11	-1.69
slab	2.0e2	4	139	158	1.09	-1.17

Simulation	Z	B	Displacement	Width	Max \vec{u}_y	$\log_{10} \text{Max } \dot{X}$
slab	2.0e2	6	48	64	0.68	-0.83
slab	2.0e2	8	32	49	0.56	-0.93
slab	2.0e2	10	27	43	0.57	-0.9
slab	4.7e2	2	143	167	1.35	-1.21
slab	4.7e2	4	89	106	1.15	-0.52
slab	4.7e2	6	25	45	0.54	-0.78
slab	4.7e2	8	14	35	0.52	-0.81
slab	4.7e2	10	9	29	0.54	-0.75
slab	1.1e3	2	102	124	1.54	-0.51
slab	1.1e3	4	56	75	1.17	-0.32
slab	1.1e3	6	16	40	0.65	-0.69
slab	1.1e3	8	-1	24	0.47	-0.73
slab	1.1e3	10	-4	19	0.5	-0.61
slab	2.6e3	2	64	87	1.75	-0.32
slab	2.6e3	4	33	56	1.35	-0.29
slab	2.6e3	6	7	33	0.92	-0.48
slab	2.6e3	8	-8	20	0.59	-0.54
slab	2.6e3	10	-15	11	0.37	-0.45
slab	6.0e3	2	34	61	2.01	-0.26
slab	6.0e3	4	14	41	1.59	-0.23
slab	6.0e3	6	-4	25	1.1	-0.34
slab	6.0e3	8	-18	11	0.53	-0.27
slab	6.0e3	10	-19	8	0.42	-0.26
slab	1.4e4	2	12	42	2.26	-0.17
slab	1.4e4	4	-2	29	1.76	-0.17
slab	1.4e4	6	-14	18	1.22	-0.19
slab	1.4e4	8	-21	9	0.62	-0.11

Simulation	Z	B	Displacement	Width	Max \vec{u}_y	$\log_{10} \text{Max } \dot{X}$
slab	1.4e4	10	-22	7	0.52	-0.08
slab	3.3e4	2	-5	29	2.46	-0.05
slab	3.3e4	4	-14	20	1.88	-0.02
slab	3.3e4	6	-22	11	1.17	0.08
slab	3.3e4	8	-25	7	0.73	0.06
slab	3.3e4	10	-24	6	0.57	0.08
slab	7.8e4	2	-17	20	2.59	0.13
slab	7.8e4	4	-24	11	1.87	0.27
slab	7.8e4	6	-27	9	1.25	0.21
slab	7.8e4	8	-27	5	0.82	0.29
slab	7.8e4	10	-27	4	0.6	0.17
slab	1.8e5	2	-27	8	2.51	0.53
slab	1.8e5	4	-28	10	1.93	0.33
slab	1.8e5	6	-30	6	1.32	0.37
slab	1.8e5	8	-29	8	0.82	0.57
slab	1.8e5	10	-28	3	0.62	0.35
slab	4.3e5	2	-31	8	2.6	0.6
slab	4.3e5	4	-32	7	1.96	0.52
slab	4.3e5	6	-32	4	1.35	0.49
slab	4.3e5	8	-30	7	0.82	0.85
slab	4.3e5	10	-29	2	0.63	0.51
slab	1.0e6	2	-34	6	2.66	0.7
slab	1.0e6	4	-35	5	1.97	0.62
slab	1.0e6	6	-34	3	1.34	0.78
slab	1.0e6	8	-30	6	0.88	1.16
slab	1.0e6	10	-29	2	0.63	0.66
slab	2.4e6	2	-37	4	2.69	0.85

Simulation	Z	B	Displacement	Width	Max \vec{u}_y	$\log_{10} \text{Max } \dot{X}$
slab	2.4e6	4	-37	3	1.98	0.87
slab	2.4e6	6	-34	7	1.34	1.06
slab	2.4e6	8	-31	5	0.8	1.26
slab	2.4e6	10	-29	2	0.62	0.85
slab	5.6e6	2	-38	4	2.7	1.12
slab	5.6e6	4	-37	3	1.99	1.07
slab	5.6e6	6	-35	3	1.31	1.05
slab	5.6e6	8	-32	5	0.78	1.41
slab	5.6e6	10	-29	2	0.69	1.13
slab	1.3e7	2	-39	7	2.71	1.41
slab	1.3e7	4	-38	2	2	1.32
slab	1.3e7	6	-36	1	1.31	1.29
slab	1.3e7	8	-32	5	0.78	1.78
slab	1.3e7	10	-29	2	0.71	1.23
slab	3.0e7	2	-39	7	2.72	1.62
slab	3.0e7	4	-38	2	2.01	1.65
slab	3.0e7	6	-36	5	1.32	1.85
slab	3.0e7	8	-32	5	0.79	2.15
slab	3.0e7	10	-29	2	0.71	1.59
slab	7.0e7	2	-39	7	2.67	2.26
slab	7.0e7	4	-38	2	2.01	2.01
slab	7.0e7	6	-36	5	1.32	2.24
slab	7.0e7	8	-32	5	0.79	2.52
slab	7.0e7	10	-29	1	0.56	1.84

Effects of Rheological Strength Contrasts on Flow Dynamics

The following simulation snapshots demonstrate the effect of the rheological activation factor B on 410 structure after 100 Ma of evolution.

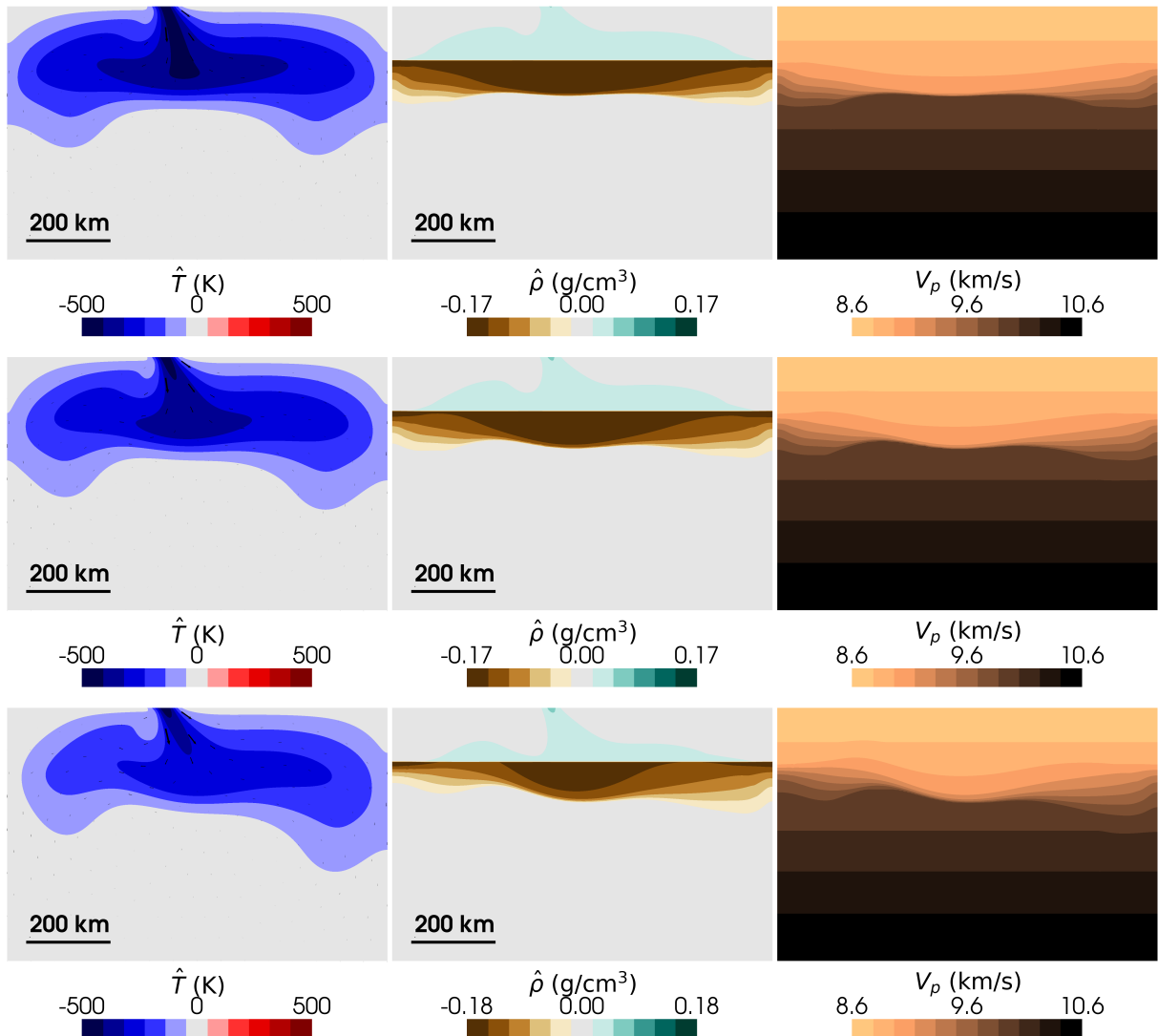


Figure 3: Slab simulations with low strength contrasts ($B = 2$) demonstrating ultra-sluggish (top row: $Z = 3.0\text{e}0 \text{ K s}^{-1}$), intermediate (middle row: $Z = 4.7\text{e}2 \text{ K s}^{-1}$), and quasi-equilibrium (bottom row: $Z = 7.0\text{e}7 \text{ K s}^{-1}$) kinetic regimes after 100 Ma evolution. Panels show dynamic temperature \hat{T} (left column), dynamic density $\hat{\rho}$ (middle column), and pressure-wave velocity V_p (right column).

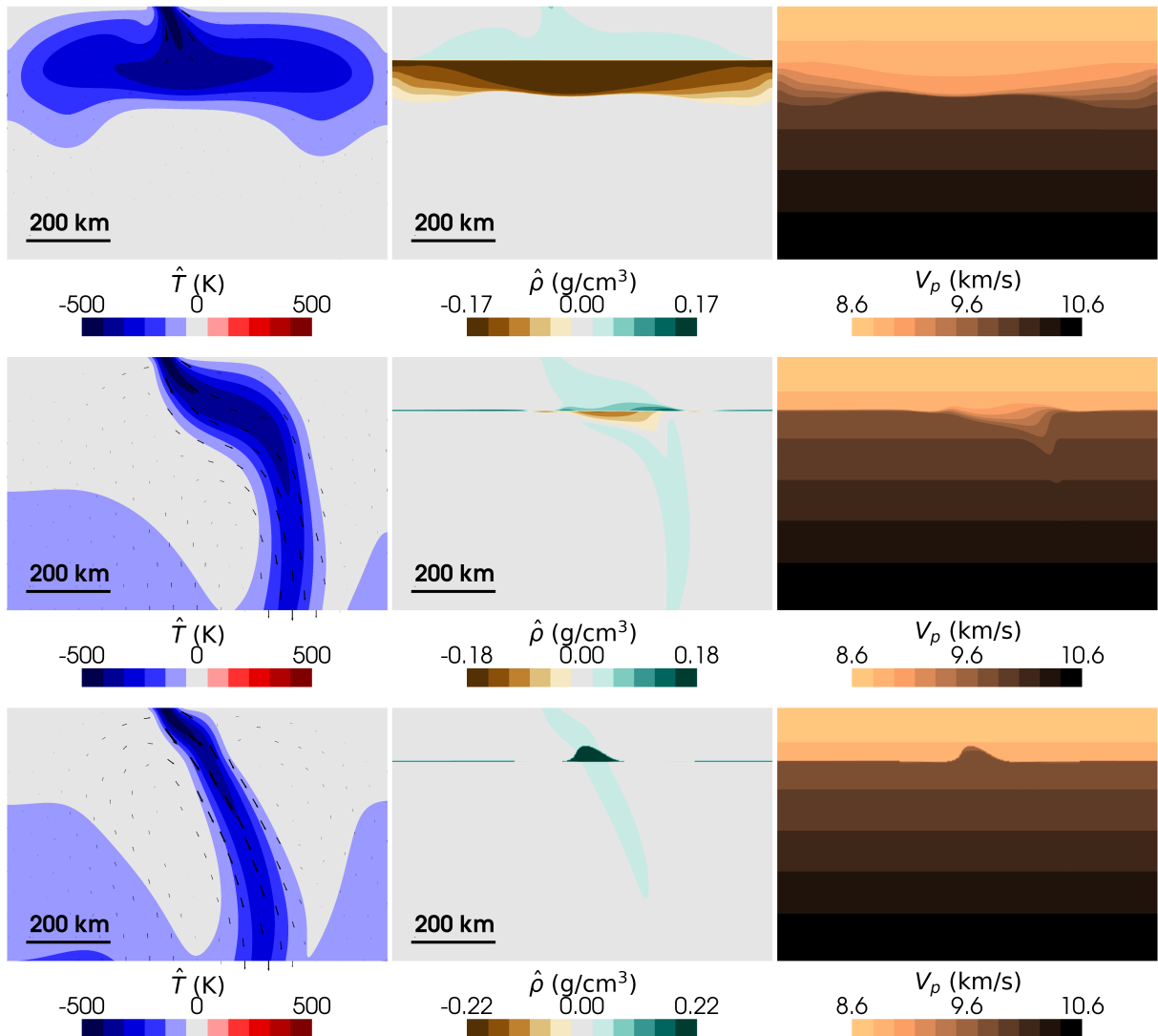


Figure 4: Slab simulations with intermediate strength contrasts ($B = 4$) showing ultra-sluggish (top row: $Z = 3.0\text{e}0 \text{ K s}^{-1}$), intermediate (middle row: $Z = 4.7\text{e}2 \text{ K s}^{-1}$), and quasi-equilibrium (bottom row: $Z = 7.0\text{e}7 \text{ K s}^{-1}$) kinetic regimes after 100 Ma evolution. Panels show dynamic temperature \hat{T} (left column), dynamic density $\hat{\rho}$ (middle column), and pressure-wave velocity V_p (right column).

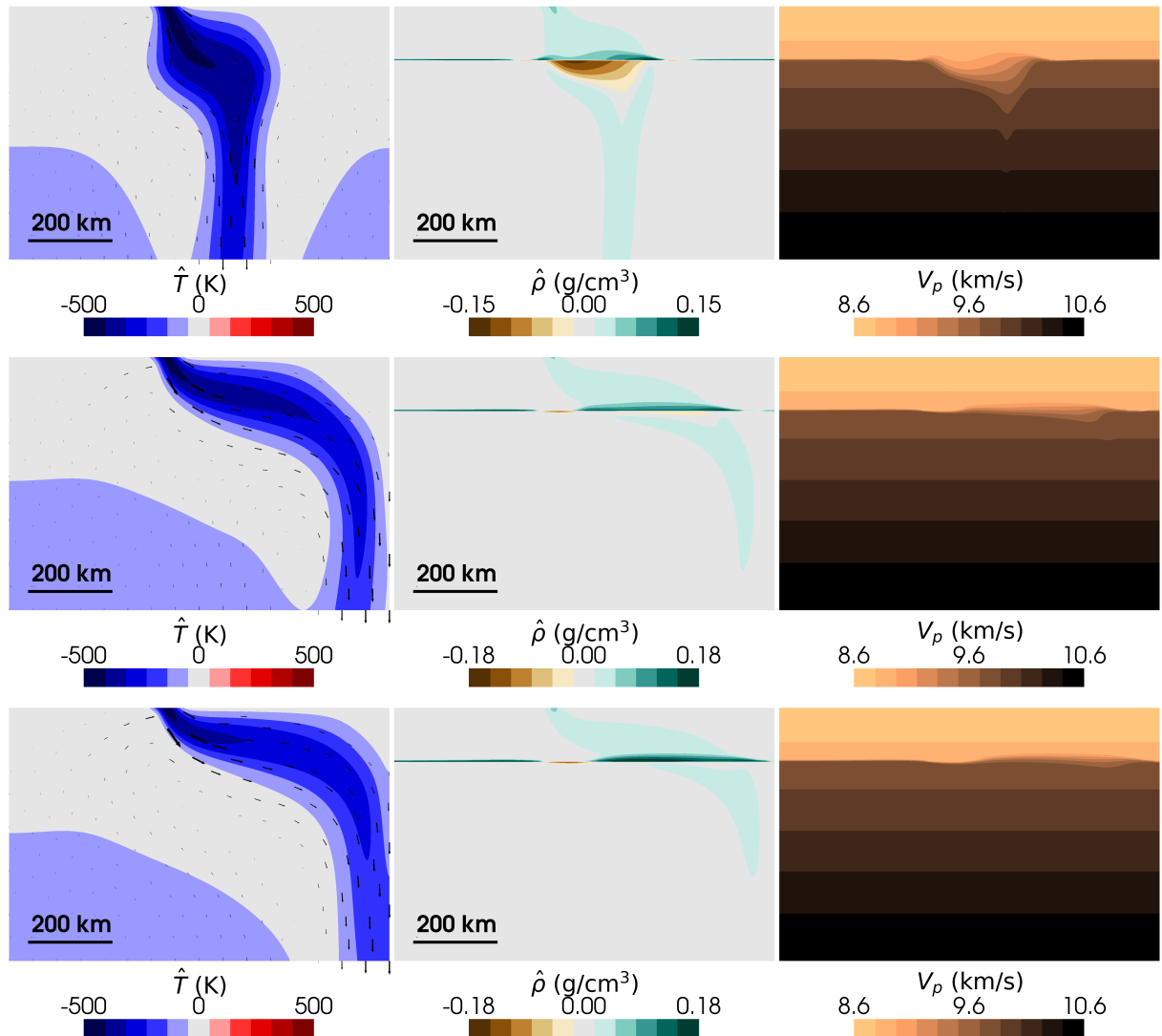


Figure 5: Slab simulations with intermediate strength contrasts ($B = 6$) demonstrating ultra-sluggish (top row: $Z = 4.7 \times 10^2 \text{ K s}^{-1}$), intermediate (middle row: $Z = 4.7 \times 10^2 \text{ K s}^{-1}$), and quasi-equilibrium (bottom row: $Z = 7.0 \times 10^7 \text{ K s}^{-1}$) kinetic regimes after 100 Ma evolution. Panels show dynamic temperature \hat{T} (left column), dynamic density $\hat{\rho}$ (middle column), and pressure-wave velocity V_p (right column).

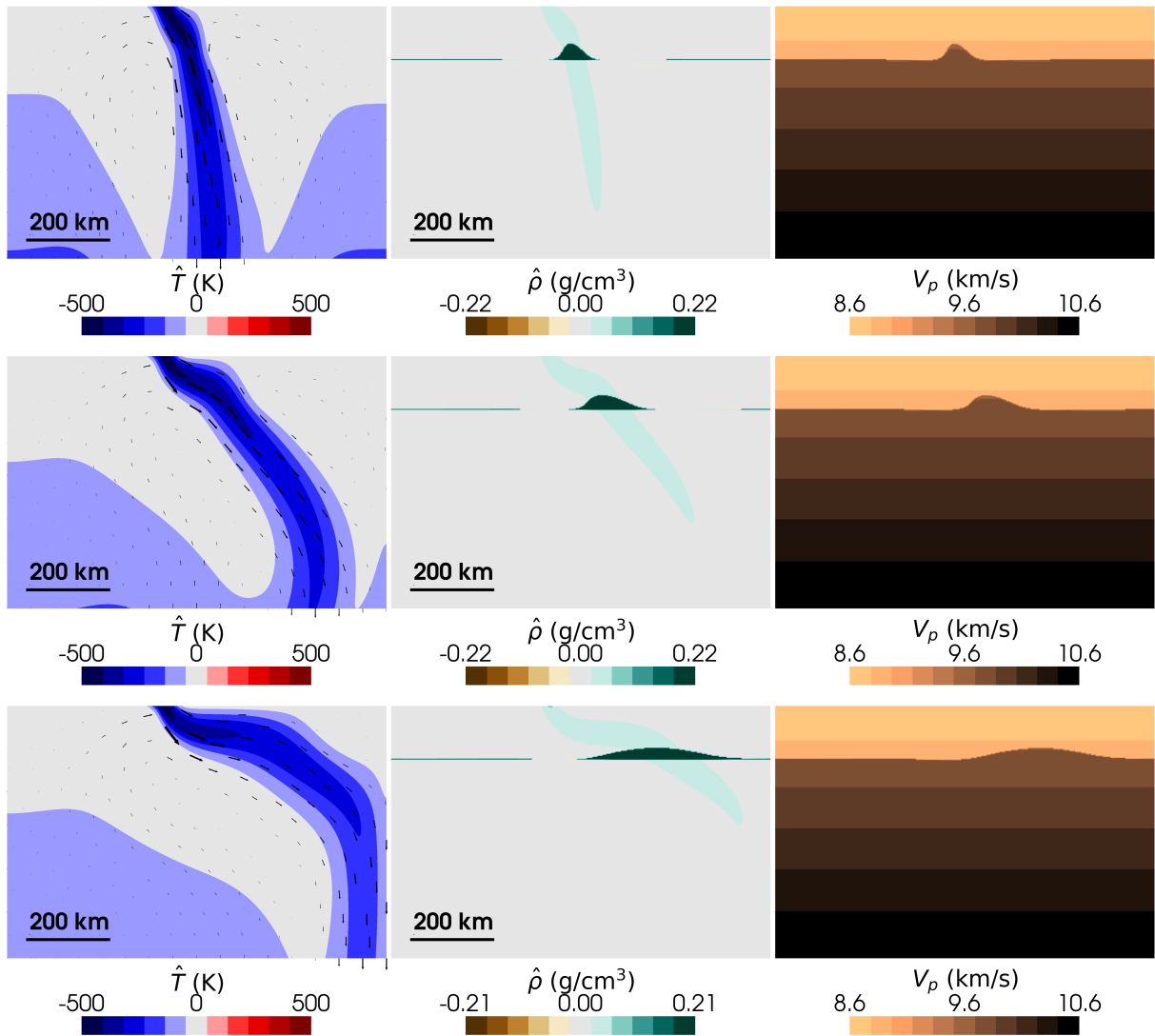


Figure 6: Slab simulations with high strength contrasts ($B = 10$) demonstrating ultra-sluggish (top row: $Z = 7.0 \times 10^7 \text{ K s}^{-1}$), intermediate (middle row: $Z = 4.7 \times 10^2 \text{ K s}^{-1}$), and quasi-equilibrium (bottom row: $Z = 7.0 \times 10^7 \text{ K s}^{-1}$) kinetic regimes after 100 Ma evolution. Panels show dynamic temperature \hat{T} (left column), dynamic density $\hat{\rho}$ (middle column), and pressure-wave velocity V_p (right column).

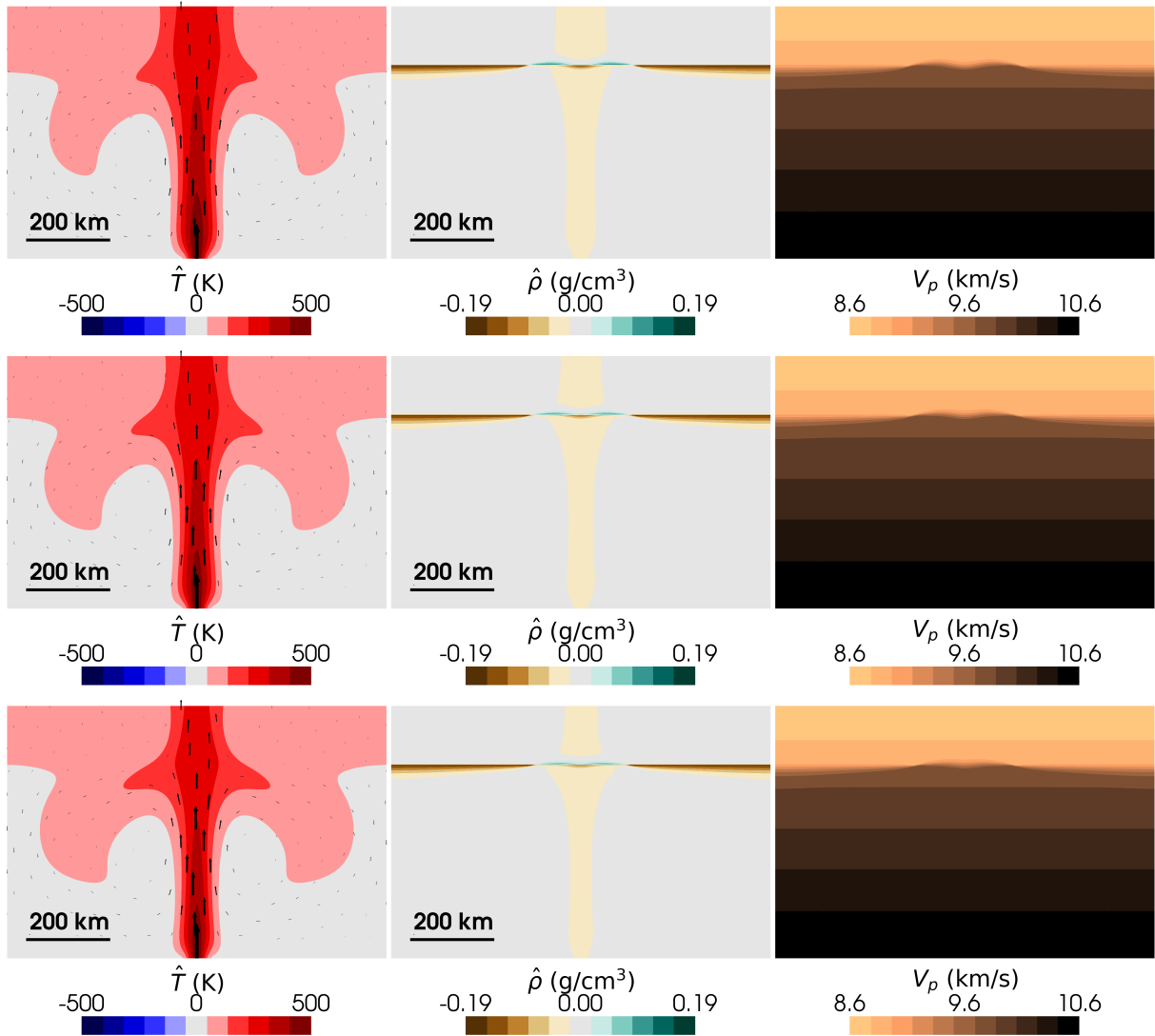


Figure 7: Plume simulations with low strength contrasts ($B = 2$) demonstrating ultra-sluggish (top row: $Z = 3.0\text{e}0 \text{ K s}^{-1}$), intermediate (middle row: $Z = 4.7\text{e}2 \text{ K s}^{-1}$), and quasi-equilibrium (bottom row: $Z = 7.0\text{e}7 \text{ K s}^{-1}$) kinetic regimes after 100 Ma evolution. Panels show dynamic temperature \hat{T} (left column), dynamic density $\hat{\rho}$ (middle column), and pressure-wave velocity V_p (right column).

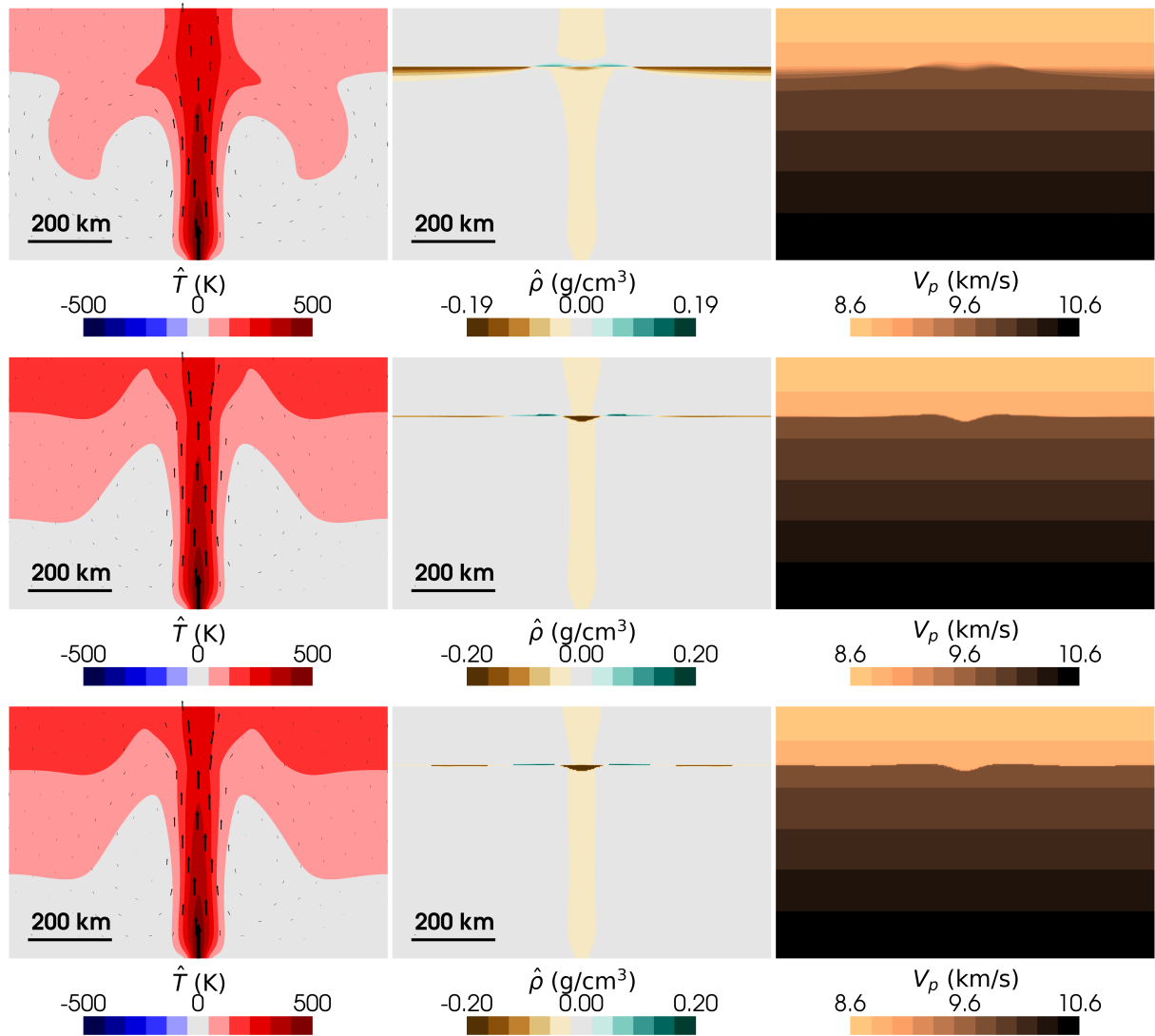


Figure 8: Plume simulations with intermediate strength contrasts ($B = 4$) showing ultra-sluggish (top row: $Z = 3.0 \text{e}0 \text{ K s}^{-1}$), intermediate-sluggish (middle row: $Z = 4.7 \text{e}2 \text{ K s}^{-1}$), and quasi-equilibrium (bottom row: $Z = 7.0 \text{e}7 \text{ K s}^{-1}$) kinetic regimes after 100 Ma evolution. Panels show dynamic temperature \hat{T} (left column), dynamic density $\hat{\rho}$ (middle column), and pressure-wave velocity V_p (right column).

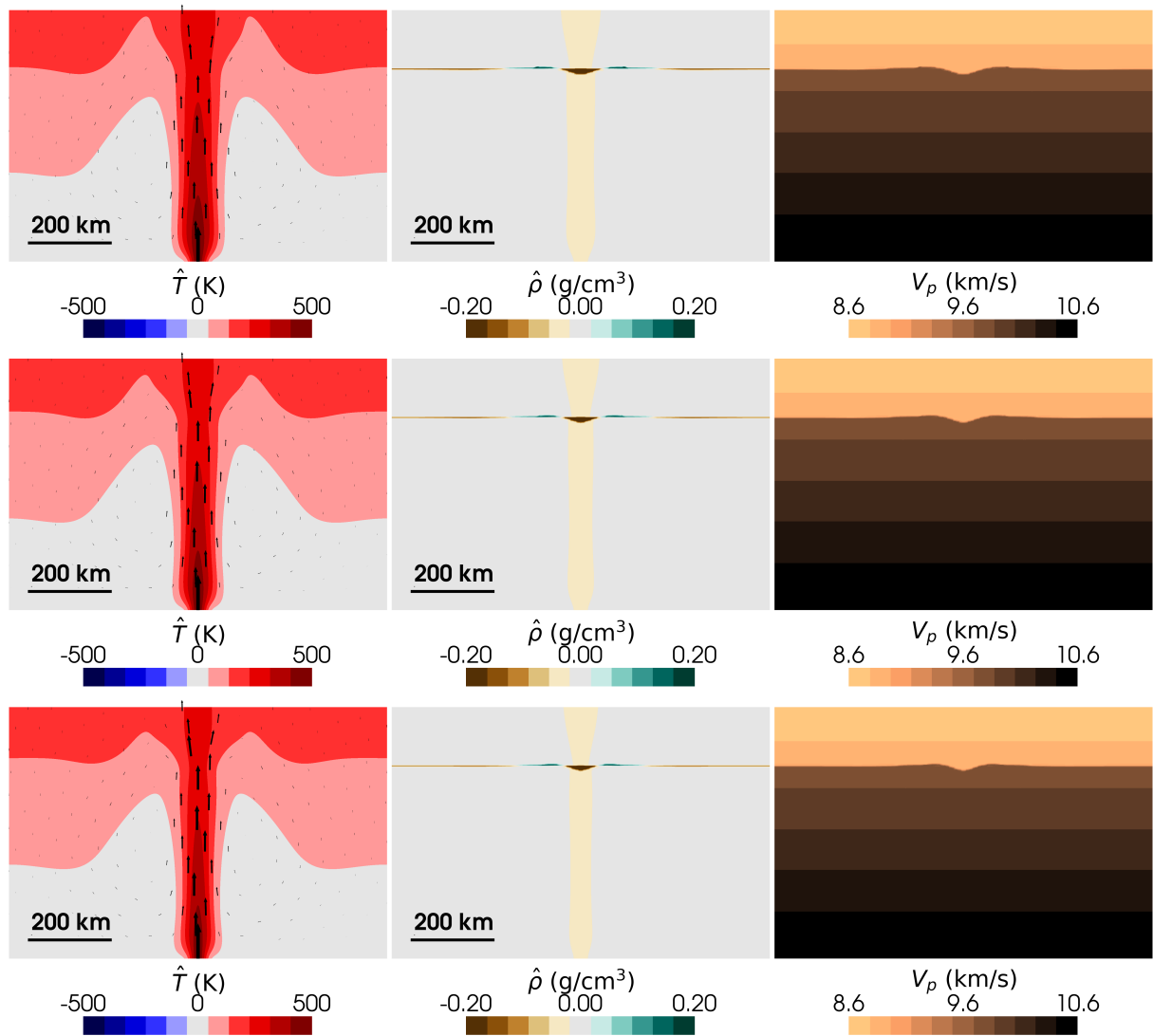


Figure 9: Plume simulations with intermediate strength contrasts ($B = 6$) demonstrating ultra-sluggish (top row: $Z = 4.7 \times 10^2 \text{ K s}^{-1}$), intermediate (middle row: $Z = 4.7 \times 10^2 \text{ K s}^{-1}$), and quasi-equilibrium (bottom row: $Z = 7.0 \times 10^7 \text{ K s}^{-1}$) kinetic regimes after 100 Ma evolution. Panels show dynamic temperature \hat{T} (left column), dynamic density $\hat{\rho}$ (middle column), and pressure-wave velocity V_p (right column).

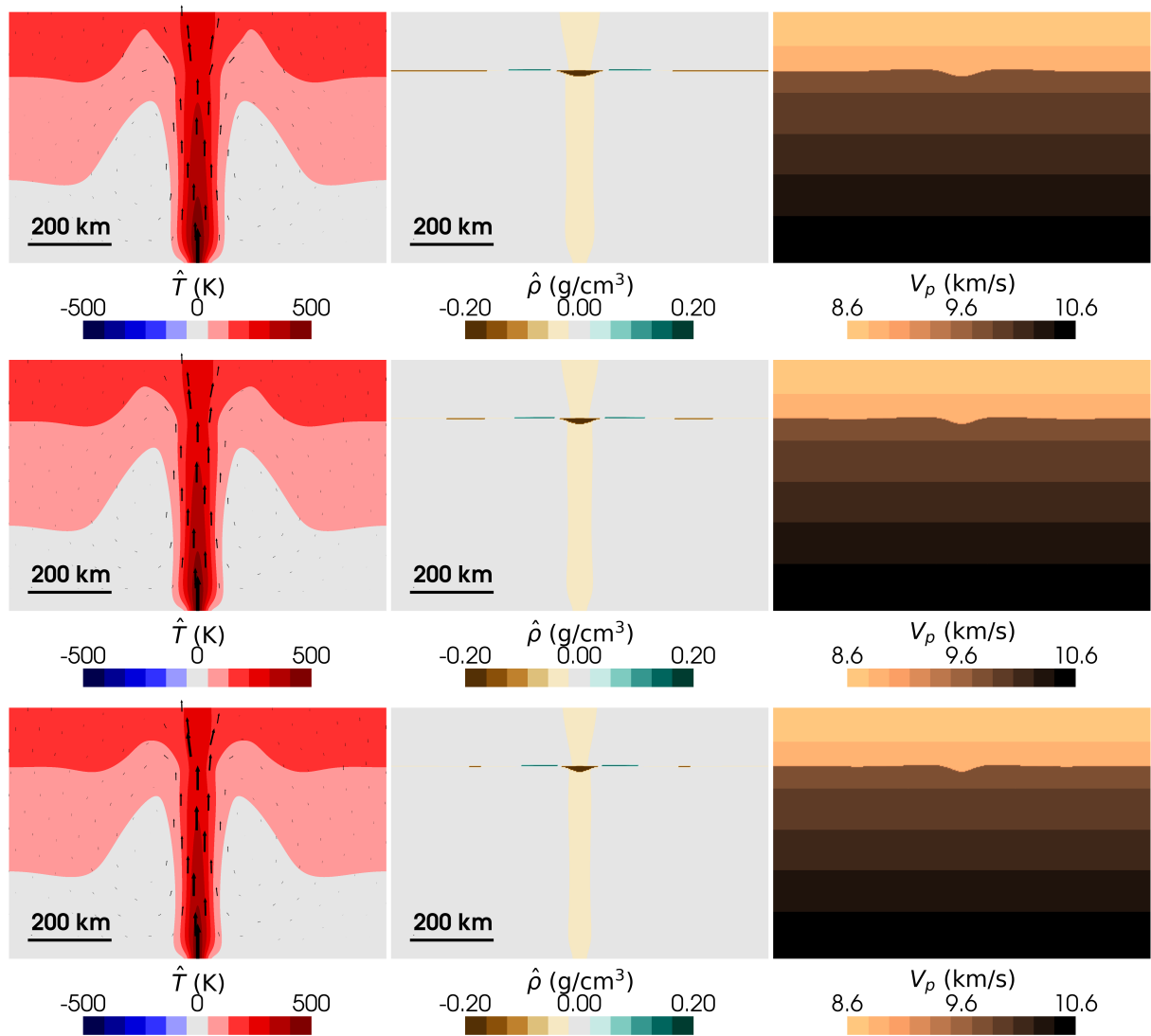


Figure 10: Plume simulations with high strength contrasts ($B = 10$) demonstrating ultra-sluggish (top row: $Z = 7.0e7 \text{ K s}^{-1}$), intermediate (middle row: $Z = 4.7e2 \text{ K s}^{-1}$), and quasi-equilibrium (bottom row: $Z = 7.0e7 \text{ K s}^{-1}$) kinetic regimes after 100 Ma evolution. Panels show dynamic temperature \hat{T} (left column), dynamic density $\hat{\rho}$ (middle column), and pressure-wave velocity V_p (right column).